JOURNAL OF OPTOELECTRONICS AND ADVANCED MATERIALS, Vol. 11, No. 11, November 2009, p. 1651 - 1655

Fractal growth of amorphous silicon crystallization induced by aluminum

ZHENGXIA TANG[a], HONGLIE SHEN[a*], HAIBIN HUANG[a], LINFENG LU[a], HONG CAI[a], JIANCANG SHEN[b]
[a]*College of Materials Science & Technology, Nanjing University of Aeronautics & Astronautics, Nanjing, 211100, China*
[b]*National Laboratory of Solid State Microstructure and Department of Physics, Nanjing University, Nanjing, 210093, China*

Glass/Al(370nm)/Al_2O_3/a-Si(600nm) stack was prepared by radio frequency magnetron sputtering and naturally oxidation. The samples were annealed at 500□ for 7 hours. After annealing, double-layered polycrystalline silicon (poly-Si) thin film was obtained. The upper layer is a continuous thin film and the lower layer consists of discontinuous dendritic crystalline grains. The fractal dimension of the dendritic crystalline grains is 1.86. Raman spectra show that the dendritic grain has high crystal quality close to single c-Si wafer.

(Received August 31, 2009; accepted November 12, 2009)

Keywords: Aluminum-induced crystallization; Polycrystalline silicon; Double layers; Fractal dimension.

1. Introduction

Polycrystalline silicon (poly-Si) thin films prepared by aluminum-induced crystallization (AIC) on low cost substrates such as glass sheets are of great interest for solar cells [1,2]. Although the AIC poly-Si is not fit for the absorber layer of solar cell due to the high aluminum content, it can be used as a seed layer for preparing large-grain poly-Si absorber layer using its excellent structural material quality [3]. 8 % efficient poly-Si solar cell has been fabricated based on AIC [4]. But as the mechanism is concerned, AIC still presents a challenge to material science. Usually the poly-Si prepared by AIC has one layer and Jens. Schneider and his group members investigated much about the theoretical mechanism of aluminum induced layer exchange (ALILE) of AIC progress [5-8]. What we report here is AIC thin film with double layer. The upper layer is continuous while the lower layer consists of discontinuous large dendritic crystalline grains. The dendritic pattern possesses scale invariance, implying a fractal structure. The properties of the double layered poly-Si and the fractal dimension were investigated. The mechanism of the fractal growth of double layers is proposed.

2. Experimental details

Corning Eagle 2000 glass was used as substrate. It was sequentially cleaned with acetone, ethanol and deionized water. 370 nm thick Al and 600 nm thick amorphous silicon (a-Si) layers were deposited by radio frequency magnetron sputtering in argon atmosphere of 1.0 Pa at 60 W and 1.5 Pa at 100 W, respectively. The Al layer was exposed to air for several hours to form an Al2O3 membrane before the a-Si layer deposition. An isothermal anneal of the glass/Al/Al2O3/a-Si stack was performed in Ar atmosphere. The furnace temperature rose from room temperature to 500 ^oC at a rate of 10 ^oC/min and kept at 500 ^oC for 7 h, following which the system was cooled down to room temperature naturally. After annealing, Al was etched off by a standard Al etching solution (80 parts H_3PO_4, 5 parts HNO_3 , 5 parts HAc and 10 parts deionized water at 55 ^oC for 15 min). Then the films were lifted off by a mixture solution of 1 part HF and 4 parts H_3PO_4 and transferred to pieces of glass for characterization.

X-ray diffraction (XRD, Bruker D8 Advance) measurements were performed using CuKα (λ = 1.5406 Å) radiation in a regular θ-2θ scan. Surface Profilermeter (ABIOS XP-1) was used to measure the thickness of the film. Raman microprobe spectroscopy (RMS, T64000) using an Ar+ laser (wavelength 514.5 nm) with a 1 μm laser spot, equipped with an optical reflectance microscopy, was used to evaluate crystalline quality. The detectable depth of the RMS in c-Si is about 100 nm. Optical transmission/reflection microscopy (OTM/ORM, Shanghai Changfang Optical Instrument Co., LTD. CMM-50) and scanning electron microscopy (SEM, LEO 1530VP) with operating voltage of 5 kV were used to characterize morphology.

3. Results

3.1 Structural property

X-ray diffraction (XRD) measurement provides information on the structural properties and crystalline quality. XRD is also possible to determine the dominant

crystal grain orientation in a polycrystalline material. The XRD measurement was performed on the sample after Al was etched off (Fig. 1). The result shows that the film is crystalline silicon with strong preferential (111) orientation. This is similar to our previous research result on the AIC poly-Si film when the Al layer was deposited by vacuum thermal evaporation [9]. In that paper, we suggested that strong preferential (111) orientation is the integrative effect of alumina membrane formed by naturally oxidizing Al layer, high annealing temperature and glass substrates. The preparation method here is similar to that except for the deposition method of Al layer, so we consider they are due to the same mechanism.

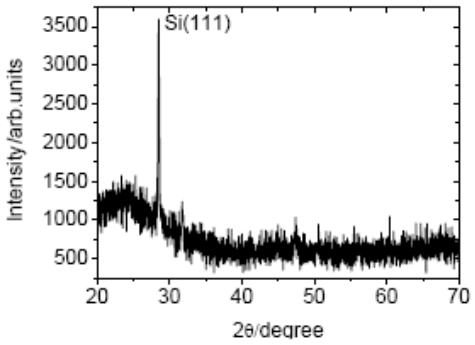

Fig. 1. XRD of the sample after Al was etched off.

3.2 Morphology

The optical microscope image provides a quick estimate of surface morphology and crystalline quality and is therefore a very useful diagnostic tool in c-Si thin film work. Fig. 2(a) and Fig. 2(b) are the ORM and OTM images of the sample taken from the glass slide before Al etching. Both the images show the dendritic grains of about 40-80 μm size. Between the dendritic grains it is silver-white in ORM and opaque in OTM, showing the existence of Al. Fig. 3(b) shows that the dendritic grains are yellow except for the orange center. And after Al was etched off, except the centre of the dendritic grains is still orange in OTM and ochroid in ORM, all the other parts are yellow both in OTM and ORM. The orange part is called in the following sections. Raman spectra in section 3.3 show that the orange protrusions are a-Si and yellow dendrites are poly-Si. Fig. 2(c) and Fig. 2(d) are the ORM images after the film was lifted off by dipping in a mixture solution of HF and H_3PO_4 and transferred onto a piece of glass. Fig. 2(c) shows that the poly-Si thin film has double layers and dendritic grains are the lower layers. Fig. 2(d) very clearly shows a single whole dendritic grain not covered by the upper layer. Fig. 2(c) shows that after Al etching the film still has double layers, but some of the upper layer is stripped off. Raman spectra in section 3.3 show that the upper layer is poly-Si film with a-Si protrusions and the lower layer consists of dendritic grains, which are corresponding to that in Fig. 2(a).

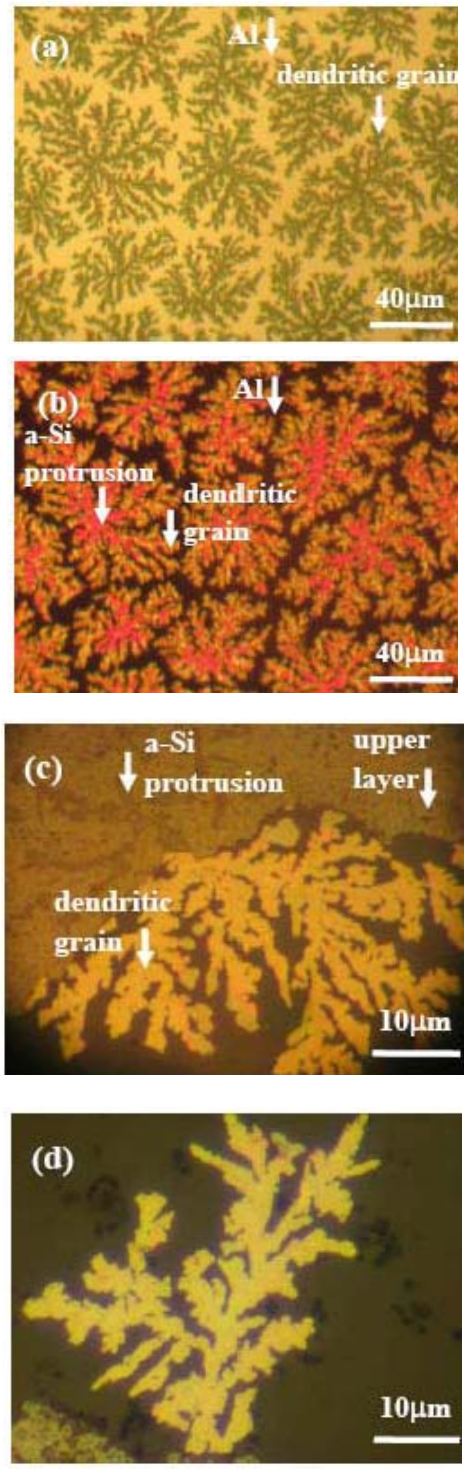

Fig. 2. (a) Optical reflection microscopy image and (b) the optical transmission microscopy image of the films taken from the glass slide after Al etching, and the optical reflection microscopy images (c) partly with and (d) without the upper layer after the film was lifted off with a mixture solution of HF and H_3PO_4.

Scanning electron microscopy (SEM) is a standard method for the investigation of the topography of a sample. Fig. 3 is the cross-section SEM of the sample before Al etching. It exhibits that the film has double layers too. The upper layer is continuous, while the lower one consists of discontinuous dendritic grain. The aluminum-induced layer exchange (ALILE) process has not completed yet and Si is partly crystallized here. What's more, the upper layer is uplifted to bend by the lower poly-Si dendrites and leaves some holes between the two layers. Oliver Nast et al. [10] investigated the crystallization of silicon during AIC process. The cross SEM in their paper shows that the poly-Si grains are rounded by Al before the ALILE process is completed.

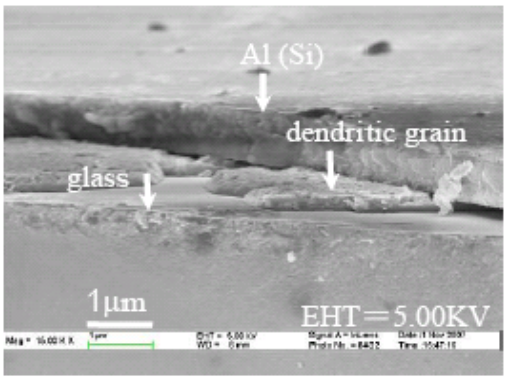

Fig. 3 Cross-section SEM of the sample before Al was etched off.

3.3 Fractal dimension of the lower dendritic grain

Fig 2(d) clearly shows a single whole dendritic grain in the lower layer. The dendritic pattern possesses scale invariance, implying a fractal structure. The simplest technique for determining the fractal dimension of an object has been termed as the "sandbox method'' [11,12]. A square with side length r is placed over a digital representation of the object. Contained within the square is a certain amount of the mass of the object, termed as M. A number of squares of increasing r are then placed concentrically over the initial square. The larger the square, the more of the object it contains. If M is plotted as a function of the side length r, a power law relation is observed, namely,

$$M = C \cdot r^{D} \quad (1)$$

Here, D is the fractal dimension and C is a constant. This equation holds as long as the size of the square is smaller than the object in question. Fig 4 shows the calculation figure of the fractal dimension of dendritic grain and Fig. 5 shows that the fractal dimension is 1.86. The fractal dimension is greater than that of the poly-Si induced by Cu (1.7) [12] and similar to that of poly-Si induced by Ag at the same annealing temperature (1.90) [13].

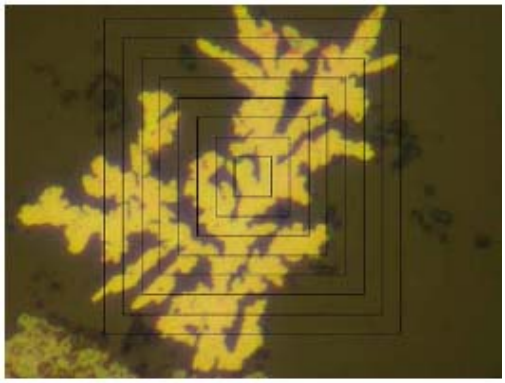

Fig. 4. Calculation figure of the fractal dimension of dendritic grain.

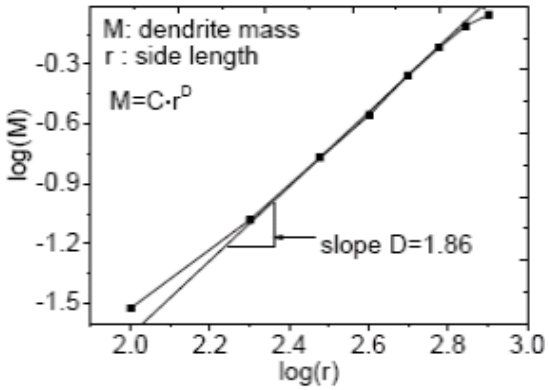

Fig. 5. Fractal dimension of dendritic grain.

3.4 Crystalline quality

As section 3.2 shows, for large-grain poly-Si thin films, the grain structure of the sample is visible in optical microscopy. It is therefore possible to select specific grains

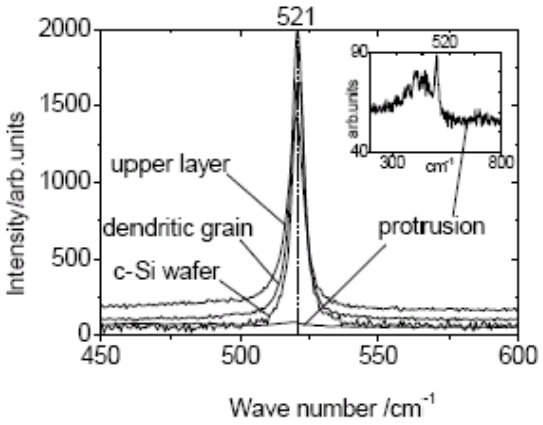

Fig. 6. Raman spectra obtained on a c-Si wafer, on the upper layer, on the dendritic grain and on the protrusion.

Table 1 Summary of the Raman spectroscopy data obtained on a CZ c-Si wafer, on the dendritic grain and on the protrusion.

Sample	Peak position / cm^{-1}	FWHM/ cm^{-1}
c-Si wafer	521	5.0
upper layer	520.3	6.8
dendritic grain	520.3	5.2
protrusion	475	69.6

with particular material quality using an optical microscope and then perform Raman measurements on these selected grains. A focused green laser beam (λ =514.5 nm) was used for these Raman measurements. Fig 6 shows the Raman spectra obtained on a CZ c-Si wafer, on the upper layer, on the dendritic grain and on the protrusion. As can be seen in Table 1, narrow Raman peaks were obtained on the upper layer, on dendritic grain and for comparison, on a CZ c-Si wafer. The peaks obtained in the protrusion on the upper layer appear at both 475 cm^{-1} and 520.3 cm^{-1} (see insert), showing the presence of a-Si phase too [14, 15]. Importantly, the full width at half maximum (FWHM) of spectrum on the dendritic grain differs only slightly from that on the CZ c-Si wafer, indicating good structural quality of the dendritic grain although the lower layer is discontinuous. The upper layer can be removed by chemical mechanical polishing (CMP) [16], high temperature (T>130 ^{o}C) ultrasonic phosphoric acid treatment [16] and selective removal by plasma etch [17].

4. Discussion

The mechanism for the formation of the double-layered poly-Si film during AIC process is schematically illustrated in Fig.7. The stack of glass/Al/Al_2O_3/a-Si is annealed at 500 ^{o}C (Step 1). During the process, Si diffuses into Al through the Al_2O_3 permeable membrane and the concentration of Si in Al layer keeps increasing. At the same time, Al diffuse into a-Si through the Al_2O_3 permeable membrane too (Step 2). The Al(Si) system is under highly nonequilibrium conditions. When the Si concentration becomes high enough, some Si begins to nucleate in Al film (Step 3). As the annealing process goes on, the formed nuclei keep growing bigger. The nuclei grow not only vertically, but also laterally. Oliver et al. proposed diffusion limiting model of AIC process [10] and the migration of Si atom is slow. Fractal structure often results from aggregation under highly nonequilibrium conditions with material transport via diffusion being the growth-determining process [18]. Obviously the formation conditions of fractal structure are satisfied here, so the nuclei form the fractal images as they grow bigger. If the lateral growth rate is high enough to make the nuclei meet together before the Al layer is uplifted by the vertically growing grains, the dendritic grains can meet each other and form a continuous poly-Si film. This can be verified by our result that the lower poly-Si layer is continuous when the sample is annealed at 550 ^{o}C for 5 h. If the lateral growth rate is not high enough, the lower poly-Si layer is discontinuous as in this paper. At the same time, Al emerges into a-Si layer and induces

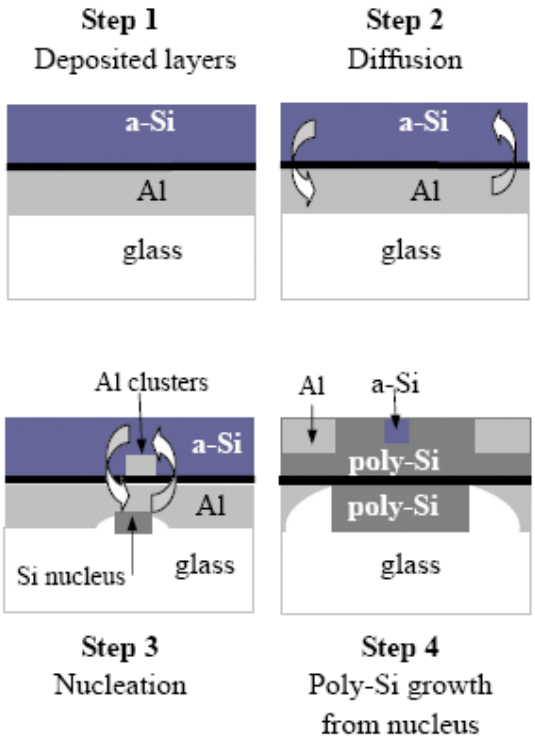

Fig. 7. Schematic diagram of the formation of the double poly-Si layers.

the upper a-Si to crystallize laterally. During the lateral crystallization process, crystalline Si forms, blocking the down diffusion of a-Si and forms the a-Si protrusions on the surface of upper poly-Si layer (Step 4).

Oliver and coworkers [10] studied the AIC process of a similar stack. They got double-layered poly-Si too, but the upper layer was a discontinuous net structure. They concluded that the best ratio of original a-Si/Al should be 1:1. Following their work, a ratio near 1:1 is usually used in AIC research. In this paper, the a-Si film was much thicker than Al film. The formation of the continuous upper layer is probably related to the thicker initial a-Si film and the slow crystallization rate during AIC process.

In fact, the 7 h annealing time is considerably longer than the usual annealing time. The direct effect of the slow rate is that the Al diffuses into the upper a-Si layer slowly giving enough time for the upper a-Si to crystallize continuously by the Al lateral induction.

5. Conclusion

Double-layered AIC poly-Si films were prepared. The film is strongly preferential (111) orientation. The lower layer consists of dendritic crystalline Si grains. A single dendritic Si grain was lifted off and analyzed. The dendritic grain implies a fractal structure and the fractal dimension measured by "sandbox method'' is 1.86. Raman spectra show that the dendritic grain has high crystal quality close to single c-Si wafer. The formation of the lower layer is explained as the traditional theory. The formation of the continuous upper layer different the usual AIC film is probably related to the thicker initial a-Si film and the slow crystallization rate during AIC process. The direct effect of the slow rate is that the Al diffuses into the upper a-Si layer slowly giving enough time for the upper a-Si to crystallize continuously by the Al lateral induction.

Acknowledgements

This work is performed with financial support from the Chinese National High Tech. "863" Program (2006AA03Z219) and Graduate Innovation Plan of Nanjing University of Aeronautics and Astronautics (BCXJ08-10).

References

[1] A.G. Aberle, J. Cryst. Growth **287**, 386 (2006).
[2] S. Gall, J. Schneider, J. Klein, K.Hübener, M. Muske, B. Rau, E. Conrad, I. Sieber, K. Petter, K. Lips, M. Stöger-Pollach, P. Schattschneider, W. Fuhs, Thin Solid Films **511-512**, 7 (2006).
[3] P. I. Widenborg, A. Straub, A. G. Aberle, J. Cryst. Growth **276**, 19 (2005).
[4] I. Gordon, L. Carnel, D. V. Gestel, G. Beaucarne, J. Poortmans, Thin Solid Films **516**, 6984 (2008).
[5] J. Schneider, A. Schneider, A. Sarikov, J. Klein, M. Muske, S. Gall, W. Fuhs, J. of Non-Cryst. Solids **352**, 972 (2006).
[6] A. Sarikov, J. Schneider, J. Klein, M. Muske, S. Gall, J. Cryst. Growth **287**, 442 (2006).
[7] M. Stöger-Pollach, T. Walter , M. Muske, S. Gall, P. Schattschneider, Thin Solid Films **515**, 3740 (2007).
[8] J. Schneider, A. Sarikov, J. Klein, M. Muskea, I. Siebera, T. Quinnb, H.S. Reehal, S. Gall, W. Fuhs, J. Cryst. Growth **287**, 423 (2006).
[9] Z. X. Tang, H. L. Shen, L. F. Lu, S. G. Song, Y. G. Yin, D. Li, J. Optoelectron. Adv. Mater. **10**, 1515 (2008).
[10] O. Nast, S.R. Wenham, J. Appl. Phys. **88**, 124 (2000).
[11] Z.Q. Wu, B. Wang, Thin film growth, Science press, Beijing, 2001, p299.
[12] S.W. Russell, J. Li, J. W. Mayer, J. Appl. Phys. **70**, 5153 (1991).
[13] B. Bian, J. Yie, B. Li, Z. Wu, J. Appl. Phys. **73**, 7402 (1993).
[14] S. Vepfek, F.A. Sarott, Phys. Rev B **36,** 3344 (1987).
[15] P. I. Widenborg, A.G. Aberle, J. Cryst. Growth **242**, 270 (2002),.
[16] D. V. Gestel, I. Gordon, L. Carnel, K. V. Nieuwenhuysen, J. D'Haen, J. Irigoyen, G. Beaucarne, J. Poortmans, Thin Solid Films **511-512**, 35 (2006).
[17] D. V. Gestel, I. Gordon, A. Verbist, L. Carnel, G. Beaucarne, J. Poortmans, Thin Solid Films **516**, 6907 (2008),.
[18] H. Röder, K. Bromann, H. Brune, K. Kern, Phys. Rev. Lett. **74**, 3217 (1995).

*Corresponding author: hlshen@nuaa.edu.cn